Submitted to Nuclear Physics

LBL-1769
Preprint

EXCITATION OF DISCRETE NUCLEAR LEVELS IN HIGH ENERGY SCATTERING PROCESSES

Gary Nixon

April 9, 1973

Prepared for the U. S. Atomic Energy Commission
under Contract W-7405-ENG-48

DISCLAIMER

Excitation of Discrete Nuclear Levels in High Energy Scattering Processes*

Gary Nixon

Lawrence Berkeley Laboratory
University of California
Berkeley, California 94720

April 9, 1973

ABSTRACT

The excitation of discrete nuclear levels in inelastic high energy scattering is examined using an extension of Glauber's diffraction theory. For T = 0 levels a simple nuclear model is introduced to obtain predictions for the excitation of collective nuclear levels which should be useful in interpreting future experiments. The particular case of (p,p') scattering to the 4.4 and 9.6 MeV levels in C^{12} is discussed and both the absolute magnitudes and the positions of diffraction minima obtained are in good agreement with experimental data. Excitation of T = 1 levels by the photoproduction of charged pions in C^{12} is computed using a particle-hole description for the nuclear states. The departure of this process from simple Fermi gas model predictions as seen in SLAC experiments is explained.

* This work was supported by the U. S. Atomic Energy Commission.

In the past twenty years much information has been obtained on the ground and excited states of a wide variety of nuclei. For example, much has been learned about the systematics of the ground state charge density using the known electromagnetic interaction of electrons. Experiments with hadronic probes have been more difficult to interpret as it has not been possible to easily and clearly separate the effects due to nuclear structure and those due to the scattering mechanism. At high energies, however, the theoretical treatment of hadron-nuclear scattering is very much simpler than at low energies. The theoretical framework used to analyze many high energy scattering experiments is the multiple scattering theory [1] of R. J. Glauber and is basically an extension of Fraunhofer diffraction theory to many-body targets. It is now realized that the effects of ground state nuclear correlations on coherent processes are small [2] and these reactions are of limited usefulness in an investigation of nuclear structure. While many workers [3,4,5] have looked into the incoherent cross section summed over final nuclear states the excitation of discrete nuclear levels has received much less attention. Our main purpose here will be to apply diffraction theory to the excitation of discrete levels. Although our results are general and would apply to the scattering of most hadrons, we will concentrate mainly on those processes for which there exists high energy data. For guidance and as check on the use of the diffraction theory we will use nuclear transition densities obtained from inelastic electron scattering data, leaving no free parameters.

The nuclear scattering amplitude, as given by the diffraction theory, can be written in a form which emphasizes multiple scattering [1]. For an A-body target with initial wavefunction u_i and final wavefunction u_f:

$$F_{fi}(q) = \left(\frac{k'}{k}\right)^{\frac{1}{2}} \langle u_f|\hat{F}|u_i\rangle \qquad (1)$$

$$\hat{F} \equiv \frac{k}{2\pi i}\int d^2b\, e^{-i\vec{q}\cdot\vec{b}}\left\{\prod_{j=1}^{A}\Big(1 - \Gamma_j(\vec{b} - \vec{s}_j)\Big) - 1\right\} \qquad (2a)$$

$$= \frac{k}{2\pi i}\int d^2b\, e^{-i\vec{q}\cdot\vec{b}}\Big\{-\Gamma_1 - \Gamma_2 - \cdots - \Gamma_A + \Gamma_1\Gamma_2$$

$$+ \Gamma_1\Gamma_3 + \cdots + (-1)^A\,\Gamma_1\cdots\Gamma_A\Big\} \qquad (2b)$$

where $\vec{k},\vec{k}'$ are the incident and final momenta, $\vec{q} = \vec{k}' - \vec{k}$ is the momentum transfer, $\vec{b}$ is the impact parameter, and $\vec{s}_j \equiv \vec{x}_j - \hat{k}z$ the transverse coordinate of the jth nucleon. The profile functions $\Gamma_j \equiv \Gamma_j(\vec{b} - \vec{s}_j)$ are given in terms of the elementary projectile jth nucleon scattering amplitude $f_j(\vec{q})$ by

$$\Gamma_j(\vec{b}) = \frac{1}{2\pi i k}\int e^{i\vec{q}\cdot\vec{b}} f_j(\vec{q})\, d^{(2)}q \qquad (3)$$

and are related to the phase shifts $\chi_j(\vec{b})$ by $\Gamma = 1 - e^{i\chi}$. In the expression Eq. (2b) the profile functions are interpreted as the "elementary" scattering amplitudes, or "vertices." The terms with a single amplitude correspond to single scattering events, those with two amplitudes to double scattering, and so on. Glauber [1] first noted that Eq. (1) satisfies the optical theorem when the projectile-nucleon interaction can be described by real phase shifts as would be

the case if no inelastic channels were open to the projectile. At high energies, however, it is believed that, for most processes, the elementary amplitudes are purely imaginary and consequently the phase shifts are imaginary. In this case also the use of the scattering operator in Eq. (2a) for inelastic scattering $i \neq f$ is consistent with its use for elastic scattering. Although this observation is not new [6] it does not appear to be widely known and is therefore given here. For imaginary f_j profile functions Γ_j are real and the optical theorem gives

$$\sigma_T = \frac{4\pi}{k}\,\mathrm{Im}\,F_{ii}(q = 0)$$

$$= -2\int d^2b\left\langle u_i\left|\left[\prod_{j=1}^{A}(1 - \Gamma_j) - 1\right]\right|u_i\right\rangle \qquad (4)$$

$$= \int d^2b\left|\left\langle u_i\left|\prod_{j=1}^{A}(1 - \Gamma_j) - 1\right|u_i\right\rangle\right|^2$$

$$+ \int d^2b\left\{\left\langle u_i\left|\left[\prod_{j=1}^{A}(1 - \Gamma_j) - 1\right]^2\right|u_i\right\rangle - \left[\left\langle u_i\left|\left(\prod_{j=1}^{A}(1 - \Gamma_j) - \right)\right|u_i\right\rangle\right]^2\right\}$$

$$+ \int d^2b\left\{-2\left\langle u_i\left|\left(\sum_{j=1}^{A}(1 - \Gamma_j) - 1\right)\right|u_i\right\rangle\right.$$

$$\left. - \left\langle u_i\left|\left[\prod_{j=1}^{A}(1 - \Gamma_j) - 1\right]^2\right|u_i\right\rangle\right\} .$$

Note that the first term is just the total elastic cross section. Inserting a complete set of nuclear states in the first part of the second term yields

$$\sigma_T = \sigma_{ELASTIC} + \sum_{n \neq i} \int d^2b \left[\left\langle u_n \middle| \left(\prod_{j=1}^{A} (1 - \Gamma_1) - 1 \right) \middle| u_i \right\rangle \right]^2$$

$$+ \int d^2b \left\langle u_i \middle| \left(1 - \left[\prod_{j=1}^{A} (1 - \Gamma_j) \right]^2 \right) \middle| u_i \right\rangle \quad .$$

The last term involves the ground state only and is the contribution from all inelastic channels in the elementary process. The second term involves excited nuclear states and is the contribution from all nuclear excitations. The important point is that it contains the same transition operator as does the elastic contribution.

The nuclear scattering amplitude as given by Eq. (1) are difficult to use as they are $3A + 2$ dimensional integrals. We know, however, that for the case of elastic coherent scattering, one can greatly simplify the calculation with the introduction of an equivalent or optical potential [7]. Consider the following expansion for $\rho_t^{(A)}(\vec{x}_1 \cdots \vec{x}_A) \equiv u_f^*(\vec{x}_1 \cdots \vec{x}_A)\, u_i(\vec{x}_1 \cdots \vec{x}_A)$

$$\rho_t^{(A)}(\vec{x}_1 \cdots \vec{x}_A) = \frac{1}{(A-1)!} S[\rho_t(\vec{x}_1)\, \rho_0(\vec{x}_2) \cdots \rho_0(\vec{x}_A)] + \cdots \qquad (5)$$

where

$$\rho_t(\vec{x}) \equiv \int d\vec{x}_2 \cdots d\vec{x}_A\, \rho_t^{(A)}(\vec{x}_1 \cdots \vec{x}_A)$$

$$\rho_0(\vec{x}) \equiv \int d\vec{x}_2 \cdots d\vec{x}_A\, u_i^*(\vec{x}_1 \cdots \vec{x}_A)\, u_i(\vec{x}_1 \cdots \vec{x}_A)$$

and where S symmetrizes over all the arguments $\vec{x}_1 \cdots \vec{x}_A$. Equation (5) is the first term in an exact expansion of the A-body transition density $\rho_t^{(A)}$ and has the properties that it is symmetric and correctly reproduces the off-diagonal matrix elements of all one-body operators [see also Refs. [7] and [8]]. The neglected terms in the expansion contain two-, three-, and up to A-body correlations in the transition density. Clearly, we have neglected any difference between the ground state single-particle density and the excited state single-particle density

$$\rho_f(\vec{x}) \equiv \int d\vec{x}_2 \cdots d\vec{x}_A\, u_f^*(\vec{x}_1 \cdots \vec{x}_A)\, u_f(\vec{x}_1 \cdots \vec{x}_A) \quad .$$

As we will see below [see Eq. (6)], the one-body character of the first term in Eq. (5) will mean its use corresponds to the assumption that the nuclear transition is direct, i.e., takes place during one of the scatterings. The rest of the scatterings serve to provide only an absorption factor.

Inserting Eq. (5) into Eq. (1) yields:

$$F_{fi} = \left(\frac{k'}{k}\right)^{\frac{1}{2}} \left(\frac{-k}{2\pi i}\right) \int d^2b\, e^{-i\vec{q}\cdot\vec{b}}\, A \int d\vec{x}\, \rho_t(\vec{x})\, \Gamma(\vec{b} - \vec{s})$$

$$\times \left[1 - \int d\vec{x}\, \rho_0(\vec{x})\, \Gamma(\vec{b} - \vec{s}) \right]^{A-1} \qquad (6)$$

for which $A \gg 1$ becomes

$$F_{fi} = \left(\frac{k'}{k}\right)^{\frac{1}{2}} \left(\frac{-k}{2\pi i}\right) \int d^2b\, e^{-i\vec{q}\cdot\vec{b}}\, A \int d\vec{x}\, \rho_t(\vec{x})\, \Gamma(\vec{b} - \vec{s})$$

$$\times\ e^{-A\int d\vec{x}\rho_0(\vec{x})\Gamma(\vec{b}-\vec{s})} \quad . \qquad (7)$$

When the range of Γ (that is, the range of the projectile-nucleon interaction) is small compared to nuclear dimensions we get:

$$F_{fi} = \left(\frac{k'}{n}\right)^{\frac{1}{2}}\left(\frac{-k}{2\pi i}\right)\int d\bar{x}\; e^{-i\vec{q}\cdot\vec{b}}\; v_t(\vec{x})\; e^{-\frac{i}{2k}\int_{-\infty}^{\infty} dz'\, V_{OPT}(\vec{b},z')} \tag{8a}$$

where

$$V_{OPT}(\vec{x}) \equiv -4\pi(A-1)\, f(0)\, \rho_0(\vec{x}) \tag{8b}$$

$$v_t(\vec{x}) \equiv A\int d^2b\; \rho_t(\vec{b},z)\; \Gamma(\vec{b}-\vec{s}) \quad . \tag{8c}$$

There are several points worth noting about this result. First, the multiple scattering expression Eq. (6) contains A-1 scatterings. This reflects the fact that there is no scattering from the "vertex" which produces nuclear excitation. Second, Eq. (7) is equivalent to a distorted wave impulse calculation. Finally, the result in Eq. (6) is <u>exactly</u> equivalent to an approximation first introduced by Lee and McManus [9]. In this approximation a typical term in the multiple scattering series Eq. (1) is given by

$$\langle n|\Gamma_i\Gamma_j|0\rangle \approx \langle n|\Gamma_i|u\rangle\langle u|\Gamma_j|0\rangle + \langle n|\Gamma_i|0\rangle\langle 0|\Gamma_j|0\rangle$$

$$\approx 2\langle n|\Gamma_i|0\rangle\langle 0|\Gamma_j|0\rangle \quad .$$

<u>Inelastic Proton Scattering</u>

Our first application of the results of the diffraction theory will be to inelastic proton scattering and in particular to the highly collective excitation of the 2^+ (4.4 MeV) and 3^- (9.6 MeV) levels in $p\text{-}C^{12}$ scattering at 1.7 GeV/c. We will take all the information

necessary in Eq. (8a) from experimental data. The amplitude f which is the isoscalar proton-nucleon spin-nonflip amplitude is parametrized in the form

$$f = \frac{k\,\sigma_T}{4\pi}(\alpha + i)\; e^{-\frac{1}{2}aq^2} \tag{9}$$

where the constants are determined from experimental data. [σ = 44.25 mb, α = -0.24, a = 5.14(geV/c)$^{-2}$ for protons at 1.69 GeV/c.] The ground state matter density appearing in Eq. (8b) is taken to be the same as the charge density measured by electron scattering and is parametrized in the form

$$\rho(\vec{x}) = \rho_0\left(1 + \eta\left(\frac{x}{R}\right)^2\right)e^{-\left(\frac{x}{R}\right)^2}\;, \quad A \leq 16\;;$$

$$\rho(\vec{x}) = \rho_0\Big/\left(1 + e^{(x-R)/z}\right), \qquad A > 16 \quad . \tag{10}$$

[The parameters we need here are, for carbon [10], η = 1.25, R = 1.65 fm, for nickel [10], R = 4.1 fm, z = 0.545 fm.] The transition density ρ_t in Eq. (8c) is the same as that measured by inelastic electron scattering and, although we could take it directly from experimental data, we will first introduce a model of the nucleus as a liquid drop. The reasons for using a nuclear model are twofold. First, the model gives us some guidance about the shape of the transition density and hence allows some information about nuclear structure to be extracted from the hadron-nuclear scattering data. Second, it is hoped that when more experimental data becomes available, this model will be as useful in correlating and understanding some of the systematics of hadron scattering to discrete collective nuclear levels as it has been for electron scattering [11,12]. Note that by using <u>measured</u> transition densities we have already included nuclear center-of-mass corrections [7] as well as the nucleon's finite size.

Folowing reference [12] the matter density in the liquid drop model is given by

$$\hat{\rho}(\vec{x}) = \rho_0\, \Theta\left[a\left(1 + \sum_{\substack{\ell,m\\ \ell\geq 2}} \hat{q}_{\ell m} Y_{\ell m}(\Omega_x) - \frac{1}{4\pi}\sum_{\substack{\ell,m\\ \ell\geq 2}} |q_{\ell m}|^2\right) - |\vec{x}|\right]$$

$$\rho_0 \equiv \frac{3}{4\pi a^3}$$

where the nuclear volume is $\frac{4}{3}\pi a^3$, Θ is the Heaviside step function, and $\hat{q}_{\ell m}$ is given by

$$\hat{q}_{\ell m} = \xi_\ell\left(\hat{a}_{\ell m}\, e^{-i\omega_e t} + (-1)^m a^+_{\ell,-m}\, e^{+i\omega_e t}\right) \quad . \qquad (12)$$

The operators $a_{\ell m}$ and $a^+_{\ell m}$ are interpreted as annihilation and creation operators for the surface oscillations (surface) which have energy ω_e, parity $(-1)^\ell$, and angular momentum (ℓ,m), ξ_ℓ are the deformation parameters. The excitation energy and deformation parameters are related to the mass density μ and surface tension σ of the drop by

$$B_\ell \equiv \mu a^5/\ell \qquad C_\ell \equiv \sigma a^2(\ell - 1)(\ell + 2)$$

$$\omega_\ell^{\,2} \equiv C_\ell/B_\ell \qquad {}_\ell \equiv \left[\frac{1}{2(B_\ell C_\ell)^{\frac{1}{2}}}\right]^{\frac{1}{2}} \qquad (13)$$

where we have neglected nuclear Coulomb forces. The density given by Eq. (11) is discontinuous at the nuclear surface and is not a very good

representation of the nucleus. We expect a better representation would be given by

$$\hat{\rho}(\vec{x}) = g\left(a\left[1 + \sum_{\substack{\ell,m\\ \ell\geq 2}} \hat{q}_{\ell m} Y_{\ell m}(\Omega_x) - \frac{1}{4\pi}\sum_{\substack{\ell,m\\ \ell\geq 2}} |q_{\ell m}|^2\right] - |\vec{x}|\right) \qquad (14)$$

where g is some function that changes smoothly as x goes through the surface region [13]. For small deformations we get

$$\rho_t(\vec{x}) = a\left(\frac{\partial g(r)}{\partial r}\right)_{r=a-|\vec{x}|} \left\langle f\left|\sum_{\substack{\ell m\\ \ell\geq 2}} \hat{q}_{\ell m} Y_{\ell m}(\Omega_x)\right| i\right\rangle \quad . \qquad (15)$$

In addition, when the range of Γ is not much larger than the dimension of ρ_t, numerical computation indicates that

$$v_t(\vec{x}) \approx -4\pi\, A\, f(0)\, \rho_t(\vec{x}) \qquad (16)$$

is a fairly good approximation.

In our calculation we choose densities g of the <u>form</u> used to describe electron scattering Eq. (10). The transition density will therefore depend upon four parameters B_ℓ, C_ℓ, R, η, or z. In order to get an idea of the general predictions of this model we take B_ℓ, C_ℓ as given by the semi-empirical mass formula [12] and R, η as given by elastic electron scattering. Figures 1 and 2 show S.E.M.F. results for the excitation of four single surfon levels in p-C^{12} and p-Ni^{58} scattering at 1.7 GeV/c. Several points are worth mentioning. First, as expected from a real multiple scattering theory, each level exhibits a series of diffraction minima. As in the case of elastic scattering [2], the depth of these minima is strongly dependent on α.

Second, the diffraction pattern of each level is somewhat characteristic of its angular momentum. Finally, the Blair phase rule [14] is fairly well satisfied.

The solid curves in Figures 3 and 4 display our results for the 2^+ and 3^- levels in p-C^{12} scattering at 1.7 GeV/c. Here the parameter B_ℓ, C_ℓ, η, R were obtained from the best fit to inelastic electron data [15] (solid lines in Figures 5 and 6) using the same nuclear model. For $\omega_2 = 4.4$ MeV they are $R = 1.55$ fm, $\eta = -0.5$, $B_2 = 11.86\,B_2'$, $C_2 = 1.24\,C_2'$, and for $\omega_3 = 9.6$ MeV they are $R = 1.65$ fm, $\eta = 1.0$, $B_3 = 18.72\,B_3'$, $C_3 = 2.45\,C_3'$ where the primed quantities denote the values given by the semi-empirical mass formula. Note that the inelastic electron form factors are described very well over the range of momentum transfer covered in Figures 3 and 4. It is important for comparisons of this kind that the range of momentum transfers be comparable otherwise seeming agreement with experimental data may be accidental†. The data in Figure 3 is for the 2^+ (4.4 MeV) level [17] and in Figure 4 is for the sum of the 0^+ (7.6 MeV) and 3^- (9.6 MeV) levels [17] which were too close to be experimentally separated. [If the 0^+ is a two-surfon state its cross section will be proportional to ξ^4 and will therefore be suppressed by a factor

† Our calculation is similar to one of Lee and McManus [9] who use the particle-hole wave functions of Gillet and Melkanoff [16] to compute the transition potential. Their results are similar except that they predict no diffraction minima. This is due to the fact that their wavefunctions fit the experimental electron scattering data only for values of $q^2 < 2\text{fm}^{-2}$.

of ξ^2 ($\xi \approx 0.4$) relative to the 3^- state. The agreement between calculation and experiment is fairly good. Our results indicate diffraction minima in the region $0.17 < q^2 < 0.23(\text{GeV/c})^2$. For the 2^+ level we see that possibility in the data but the 3^- data does not extend out far enough for a comparison. The dashed lines in Figures 3 and 4 give the cross section in the Born approximation and we see that agreement is not good. Clearly, rescattering plays an important role and cannot be neglected.

Charged Pion Photoproduction

In this section we will study the excitation of $T = 1$ nuclear levels by the photoproduction of charged pions in C^{12} (8 GeV). The multiple scattering operator Eq. (2a) may be generalized to include processes in which the projectile undergoes a transition. Using the results of Ref. [2] we get for pion photoproduction

$$\hat{F}_{\gamma\pi} = -\sum_{i=1}^{A} \prod_{k=i+1}^{A} \Gamma_i^{\gamma\pi}(\vec{b} - \vec{s}_i)\left(1 - \Gamma_k^{\pi N}(\vec{b} - \vec{s}_k)\right) \tag{17a}$$

$$\Gamma_i^{\gamma\pi}(\vec{b} - \vec{s}_i) = \frac{1}{2\pi i k}\int d^2q\; e^{i\vec{q}\cdot(\vec{b}-\vec{s}_i)}\, f^{(i)}_{\gamma\pi}(\vec{q}) \tag{17b}$$

and where $f^{(i)}_{\gamma\pi}(\vec{q})$ is the elementary pion photoproduction amplitude on the ith nucleon. We have neglected the extra phase in F due to the longitudinal momentum transfer $\Delta_m \approx -(m_\pi^2)/(2k)$ associated with a change in mass as it has negligible effect for photoproduction of pions in the several GeV range. In this expression there are no terms corresponding to the elastic scattering of the photon. This is because the photon is a weak probe (with mean free path ~600 fm in nuclear matter) whereas a strongly interacting particle has a mean free path small compared to nuclear dimensions. Consequently, we expect the nuclear amplitude to be dominated completely by the production process and by rescattering of the produced particle; $\Gamma^{\gamma\pi}$ is an operator on the target particles with both spin and isospin dependence. We may use the generalization of Eq. (5) which includes spin and isospin [8] to obtain

$$F = -\frac{k}{2\pi i}\int d\vec{x}\, e^{-i\vec{q}\cdot\vec{b}} \left\langle f \left| \sum_{i=1}^{A} \delta(z - z_i)\, \Gamma_i^{\gamma\pi}(\vec{b} - \vec{s}_i) \right| i \right\rangle$$

$$\times \left[1 - \int_z^\infty dz' \int d^2s'\, \rho_0(\vec{s}', z')\, \Gamma^{\pi N}(\vec{b} - \vec{s}')\right]^{A-1} \qquad (18)$$

where we are assuming $T_f = 1$, $T_i = 0$. Equation (18) can also be derived [8,18] from a pseudopotential approach under the "weak" assumption that the πN potentials do not overlap with the production potential. This expression also has the expected structure with an incoming wavefunction that includes only $A-1$ scatterings and a pion "production potential:"

$$v_{\gamma\pi}(\vec{x}) = -2ki \left\langle f \left| \sum_{i=1}^{A} \delta(z - z_i)\, \Gamma_i^{\gamma\pi}(\vec{b} - \vec{s}_i) \right| i \right\rangle . \qquad (19)$$

It may be written in a form involving an optical potential if we take the large A limit together with the usual assumption that the range of $\Gamma^{\pi N}$ is small compared to the nucleus. We then obtain

$$F = -\frac{1}{4\pi}\int d\vec{x}\, e^{-i\vec{q}\cdot\vec{b}}\, v_{\gamma\pi}(\vec{x})\, e^{\frac{i}{2k}\int_z^\infty dz'\, V_{OPT}(\vec{b}, z')} \qquad (20a)$$

$$V_{OPT}(\vec{x}) = -4\pi A\, f_{\pi N}(0)\, \rho_0(\vec{x}) \quad . \qquad (20b)$$

If, in addition, we assume the photo-pion conversion takes place in a space small compared to the dimension of the transition density, then

$$v_{\gamma\pi}(\vec{x}) = -4\pi \left\langle f \left| \sum_{j=1}^{A} \delta(\vec{x} - \vec{x}_i)\, f^{(j)}_{\gamma N \to \pi N}(0) \right| i \right\rangle \quad . \qquad (21)$$

Equation (20a) is equivalent to the assumption of a pseudopotential $\hat{v}_{\gamma\pi}$ acting in the nuclear Hilbert space which gives the correct amplitude in Born approximation for photoproduction of pions on a single nucleon:

$$\hat{v}_{\gamma\pi}(\vec{x}) = -4\pi \sum_{i=1}^{A} \delta(\vec{x} - \vec{x}_i)\, f^{(i)}_{\gamma N \to \pi N}(0) \quad . \qquad (22)$$

A calculation of the nuclear amplitude requires (1) the optical potential which we shall compute from experimental data (for pions at 8 GeV/c, $\sigma = 26$ mb, $\alpha = -0.15$) as in the last section, (2) the elementary amplitude for pion-photoproduction $f_{\gamma N \to \pi N}$ and (3) the nuclear wave functions.

In general, the nature of high energy hadron processes is an open question. However, it has been noted that [19,20,21], in the case of charged pion photoproduction, a relatively simple theoretical description (Born approximation) of $f_{\gamma\pi}$ exists which can reproduce much of the experimental data for high energies $k_j > 1$ GeV and small momentum transfer $q^2 < 2m_\pi^2$. Thus, for $f_{\gamma\pi}$ we choose a set of gauge invariant Feynman graphs, Fig. 7, which we assume play the most important part in pion photoproduction. Denoting the photon and pion four momenta by k and q and the nucleon initial and final four momenta by p_1 and p_2 the amplitude in the forward direction in the lab frame is given by

$$\hat{f}_{\gamma\pi^+} = \left[\frac{q}{k}\left(\frac{e}{4\pi}\right)^2 \frac{m}{m+k}\right]^{\frac{1}{2}} \frac{1}{\sqrt{2}} F_1\, i\vec{\sigma}\cdot\vec{\epsilon}\,\tau^- \qquad (23a)$$

$$F_1 = \left(\frac{E_{p_2}+m}{2m}\right)^{\frac{1}{2}} [Ak - Cq\cdot k - 2DP\cdot k - 2mDk] \qquad (23b)$$

where $P \equiv \frac{1}{2}(P_1 + P_2)$, $\vec{\epsilon}$ is the photon's polarization and τ^- is the isotopic spin lowering operator. The invariant amplitudes A, B, C, D computed from the Feynman diagrams [22], are found to be for π^+ production

$$A = -g\sqrt{2}\left\{\frac{1}{(P_1+k)^2+m^2}\right\}$$

$$B = -\frac{1}{q\cdot k}A \qquad (24)$$

$$C = g\sqrt{2}\,\frac{1}{2m}\left\{\frac{\mu_P - 1}{(P_1+k)^2+m^2} - \frac{\mu_N}{(P_2-k)^2+m^2}\right\}$$

$$D = g\sqrt{2}\,\frac{1}{2m}\left\{\frac{\mu_P - 1}{(P_1+k)^2+m^2} + \frac{\mu_N}{(P_2-k)^2+m^2}\right\}$$

with $\mu_P \simeq 2.79$, $\mu_n \simeq -1.91$, $g \equiv g_{\pi NN} \simeq 13.6$. It is convenient to rewrite Eq. (23a) in spherical tensor form

$$\hat{f}_{\gamma\pi^+} = \sum_{S=0}^{1}\sum_{\lambda=-S}^{S}(-1)^\lambda K_{S_1-\lambda}(\rho)\,\sigma_\lambda^S\,\tau^- \qquad (25)$$

with $\sigma_0^0 \equiv 1$ and σ_λ^1 the tensor form of the Pauli spin matrices; $\rho = 1(2)$ if the photon is polarized perpendicular (parallel) to the reaction plane and in the forward direction:

$$K_{00}(\rho) = 0 = K_{1,0}(\rho)$$

$$K_{1,1}(\rho) = F_1(\delta_{\rho 2} - i\delta_{\rho 1}) \qquad (26)$$

$$K_{1,-1}(\rho) = F_1(\delta_{\rho 2} + i\delta_{\rho 1}) \,.$$

At small momentum transfers the most important processes in π^+ photoproduction on C^{12} are the excitation of $T = 1$ levels in B^{12} which are believed to be isobaric analogs of various $T = 1$ levels of C^{12}. These latter states are just those which can be reached by inelastic electron scattering and photoexcitation. For excitation energies 15 MeV $\leq \omega \leq$ 40 MeV, these processes are dominated by the excitation of certain highly collective levels called giant resonances. To describe these levels we will use the particle-hole model [23] of Brown and Bosterli which has been successfully used to explain the giant dipole seen in photoexcitation and to interpret the data from inelastic electron scattering [12,24], muon capture [25], and inelastic proton scattering at intermediate energies [26]. The nuclear matrix element required in Eq. (21) is

$$M.E. = \left\langle f_1 T_f = 1,\ T_{fz} = -1 \left| \sum_{j=1}^{A} \delta(\vec{x} - \vec{x}_j)\, f_{\gamma\pi}^{(j)}(0) \right| i_j T_i = T_{iz} = 0 \right\rangle \qquad (27)$$

where $f_{\gamma\pi}$ is proportional to τ^-. From the Wigner-Eckart theorem we can write

$$\text{M.E.} = \begin{pmatrix} 1 & 1 & 0 \\ 1 & -1 & 0 \end{pmatrix} \Big\langle f, J_f, M_{J_f}, T_f = 1 \Big\| \sum_{j=1}^{A} \delta(\vec{x} - \vec{x}_j)\, f^{(j)}_{\gamma\pi^+}(0) \Big\|$$

$$\times \quad i, J_i, M_{J_i}, T_i = 0 \Big\rangle \tag{28}$$

(the matrix element is reduced in isospin only). Assuming Coulomb effects to be small, we can compute the reduced matrix element in Eq. (28) using the wavefunction mentioned above.

In the particle-hole model the nuclear wave functions are considered to be linear combinations of particle-hole states of given angular momentum J and isospin T:

$$\psi_{JM_JTM_T}(\bar{x}_1 \cdots \bar{x}_A) = \sum_K \alpha_{JT}^K\, \phi^K_{JM_JTM_T}(\vec{x}_1 \cdots \vec{x}_A) \tag{29}$$

where K stands for the quantum numbers $(n_1\ell_1 j_1)-(n_2\ell_2 j_2)^{-1}$ with the labels 1 for particles and 2 for holes, and where Φ stands for pure particle-hole states. The matrix element of any multiple operator M_{JT} is given by:

$$|\langle \psi_{JT} \vdots\vdots M_{JT} \vdots\vdots \psi_{J_0 T_D} \rangle|^2 = \sum_{\substack{n_1\ell_1 j_1 \\ n_2\ell_2 j_2}} \alpha_{JT}^{(n_1\ell_1 j_1)(n_2\ell_2 j_2)^{-1}}$$

$$\times \quad |\langle n_1\ell_1 j_1 \vdots\vdots M_{JT} \vdots\vdots n_2\ell_2 j_2 \rangle|^2 \tag{30}$$

where the symbol $\langle \vdots\vdots \;\; \vdots\vdots \rangle$ indicates a reduced matrix element with respect to both isotopic spin and angular momentum. The matrix elements $\langle n_1\ell_1 j_1 \vdots\vdots M_{JT} \vdots\vdots n_2\ell_2 j_2 \rangle$ are now just single particle matrix elements. We take the coefficients α_{JT}^K corresponding to the dominant $T = 1$ single particle-hole states in C^{12} from a calculation of T. W. Donnelly and which are known to give a reasonable account of inelastic electron scattering [24]. They were computed for oscillator parameter $b = 1.64$ fm and are given in Table I. The nuclear photoproduction amplitude can then be written

$$F_{\gamma\pi^+} = \int d\vec{x}\, e^{-i\vec{q}\cdot\vec{x}}\, e^{-\frac{i}{2k}\int_z^\infty dz' V_{OPT}(\vec{b},z')} \sum_{LM} Y^*_{LM}(\Omega_x)$$

$$\times \sum_{s,\lambda} (-1)^\lambda K_{s,-\lambda}(\rho)(-1)^{L+M_f+S}(2J_f+1)^{\frac{1}{2}} \begin{pmatrix} L & S & J_f \\ M & \lambda & -M_f \end{pmatrix} F^{LSJ_f}(x) \tag{31}$$

where

$$F^{LSJ} = \frac{1}{b^3}\left\{C_1 \frac{x}{b} + C_2\left(\frac{x}{b}\right)^3\right\} e^{-\left(\frac{x}{b}\right)^2} \quad \text{for odd parity states}$$

$$= \frac{1}{b^3}\; D\left(\frac{x}{b}\right)^2 e^{-\left(\frac{x}{b}\right)^2} \quad \text{for even parity states}$$

and where the coefficients C_1, C_2, and D are given in Table II. In Fig. 8 we show the differential nuclear cross section for the excitation of all levels together with experimental data from Ref. [27]. Figure 9 gives the cross section as a function of excitation energy for different momentum transfers. Donnelly finds that to account for inelastic electron data, the form factors for odd parity states should be reduced by $1/\sqrt{2}$ and those for even parity by $1/2$: this has been done in Figs. 8 and 9. The dashed line gives the contribution from odd parity states, and the solid line is the result including all states. For comparison, we also give the result of the Fermi gas model and note that the departure of experiment from this model at small momentum transfer is accounted for by our particle-hole calculation. Finally, we mention that we expect the contribution from negative parity states to be fairly systematic from nucleus to nucleus while the positive parity ones may be important only in C^{12}. However, this would not affect any of our results above as the contribution from these states is small.

Conclusions

We have looked at inelastic processes to see what could be learned about nuclear structure. For $T = 0$ levels we used a simple nuclear model to obtain predictions for the excitation of collective nuclear oscillations which should prove useful both as a guide and in interpreting the experiments which one can look forward to with the new meson factory. Further, we showed that in the case of (p,p') to the 4.4 MeV and 9.6 MeV levels in C^{12}, where there is data available, the model together with diffraction theory correctly describes the data; and we predicted both absolute magnitude and position of two diffraction minima when the transition densities were taken from inelastic electron scattering. For the excitation of $T = 1$ levels by the photoproduction of charged pions on C^{12} we used the particle-hole model of nuclear excitation. The excitation of these discrete nuclear levels is the most important process at high incident energy and small momentum transfer, and we have computed it for the

first time. The calculation is able to explain the departure of this process from a simple Fermi gas model prediction as seen in recent SLAC experiments. For both $T = 0$ and $T = 1$ levels we have seen that the information on nuclear structure present in the data available today is essentially the same as that obtained by electron scattering.

References

1) R. J. Glauber, Lectures in Theoretical Physics, Vol. 1 (Wiley Interscience, New York, 1959), p. 315; High Energy Physics and Nuclear Structure, S. Devens, ed. (Plenum Press, New York, 1970), p. 207.

2) E J. Moniz and G. D. Nixon, Ann. Phys. 67 (1971) 222.

3) K. S. Kolbig and B. Margolis, Nucl. Phys. B6 (1968) 85.

4) R. J. Glauber, in "High Energy Physics and Nuclear Structure", p. 311, G. Alexander, ed. (North-Holland, Amsterdam, 1967).

5) J. S. Trefil, Nucl. Phys. B11 (1969) 330.

6) W. Czyz, private communication.

7) L. L. Foldy and J. D. Walecka, Ann. Phys. 56 (1970) 268.

8) G. D. Nixon, Ph.D. Thesis, Stanford University, 1971 (unpublished).

9) H. K. Lee and H. McManus, Phys. Rev. Letters 20 (1968) 337.

10) R. Hofstadter and H. R. Collard in Landolt-Bornstein, Group 1, Vol. 2 (Springer Verlag, Berlin, 1967).

11) J. D. Walecka, Phys. Rev. 126 (1962) 653 and 663.

12) T. deForest, Jr. and J. D. Walecka, Adv. in Phys. 15 (1966) No. 57, 1.

13) L. J. Tassie, Aust. J. Phys. 9 (1956) 407.

14) N. Austern and J. S. Blair, Ann. of Phys. 33 (1965) 15.

15) H. Crannel, Phys. Rev. 148 (1966) 1107.

16) V. Gillet and M. A. Melkanoff, Phys. Rev. 133 (1964) B1190.

17) J. L. Friedes, H. Palevsky, R. J. Sutter, G. W. Bennett, G. J. Igo, W. D. Simpson, and D. M. Corley, Nucl. Phys. A104 (1967) 294.

18) E. J. Moniz, Ph.D. Thesis, Stanford University, 1971 (unpublished).

19) B. Richter, Proceedings 1967 International Symposium in Electron and Photon Interactions at High Energies, Stanford Linear Accelerator Center, p. 309.

20) R. Diebold, High Energy Physics Conference, Boulder, Colorado (1969).

21) H. Harari, Proceedings 1967 International Symposium on Electron and Photon Interactions at High Energies, Stanford Linear Accelerator Center, 1967, p. 337.

22) J. D. Walecka and P. A. Zucker, Phys. Rev. 167 (1968) 1479.

23) G. E. Brown and M. Bosterli, Phys. Rev. Letters 3 (1959) 472.

24) T. W. Donnelly, Phys. Rev. C1 (1970) 833.

25) L. L. Foldy and J. D. Walecka, Nuovo Cimento 34 (1964) 1026.

26) H. K. Lee and H. McManus, Phys. Rev. 161 (1967) 1087.

27) A. M. Boyarski et al., SLAC-PUB-671, Stanford Linear Accelerator Center, Stanford, California (1969).

Table I. Energies and Wave Functions for T = 1 States with b = 1.64 fm

Level	J^{π}	Energy (MeV)	$(2s_{1/2})(1p_{3/2})^{-1}$	$(1d_{3/2})(1p_{3/2})^{-1}$	$(1d_{5/2})(1p_{3/2})^{-1}$	$(1p_{1/2})(1s_{1/2})^{-1}$	$(1p_{1/2})(1p_{3/2})^{-1}$
1	0^-	25.53			0.936	-0.352	
2	0^-	35.45			0.353	0.936	
3	1^-	19.52	0.978	-0.165	0.129	-0.016	
4	1^-	23.09	0.188	0.958	-0.192	0.095	
5	1^-	24.89	-0.089	0.229	0.940	-0.238	
6	1^-	35.55	-0.025	-0.040	0.252	0.967	
7	2^-	18.80	0.939	-0.344	-0.024		
8	2^-	20.60	0.337	0.931	-0.140		
9	2^-	23.83	0.070	0.124	0.990		
10	3^-	19.24		0.992	0.123		
11	3^-	25.05		-0.123	0.992		
12	4^-	20.17		1.0			
13	1^+						1.0
14	2^+						1.0

Table II. Coefficients for Nuclear Form Factors

Level	$J_f^{\pi_f}$	Form Factor F^{LSJ_f}	C_1	C_2	D
1	0^-	F^{110}	-0.366	0.711	
2	0^-	F^{110}	0.973	0.267	
3	1^-	F^{111}	0.705	-0.476	
3	1^-	F^{101}	-1.007	0.555	
4	1^-	F^{111}	0.219	0.199	
4	1^-	F^{101}	-0.252	0.731	
5	1^-	F^{111}	-0.267	0.660	
5	1^-	F^{101}	0.235	-0.111	
6	1^-	F^{111}	0.802	0.135	
6	1^-	F^{101}	-0.554	-0.090	
7	2^-	F^{312}	0.0	-0.033	
7	2^-	F^{112}	-1.196	0.623	
8	2^-	F^{312}	0.0	0.144	
8	2^-	F^{112}	-0.429	0.714	
9	2^-	F^{312}	0.0	-0.246	
9	2^-	F^{112}	-0.089	0.333	
10	3^-	F^{313}	0.0	-0.145	
10	3^-	F^{303}	0.0	-0.264	
11	3^-	F^{313}	0.0	-0.430	
11	3^-	F^{303}	0.0	0.421	
12	4^-	F^{514}	0.0	0.0	
12	4^-	F^{314}	0.0	-0.609	

Table II continued next page

Table II continued

Level	$J_f^{\pi_f}$	Form Factor F^{LSJ_f}	C_1	C_2	D
13	1^+	F^{211}			-0.283
13	1^+	F^{011}			0.800
14	2^+	F^{212}			-0.658
14	2^+	F^{202}			0.537

FIGURE CAPTIONS

Fig. 1. Proton-C^{12} inelastic cross sections in the center of mass frame for the 2^+, 3^-, 4^+, and 5^- levels. Nuclear parameters derived from S.E.M.F. σ = 44.25 mb, α = -0.24, k = 1.7 GeV/c.

Fig. 2. Proton-Ni^{58} inelastic cross sections in the center of mass frame for the 2^+, 3^-, 4^+, and 5 levels. Nuclear parameters derived from S.E.M.F. σ = 44.25 mb, α = -0.24, k = 1.7 GeV/c.

Fig. 3. Cross section for the excitation of the 4.4 (2^+) MeV level in C^{12} with protons at 1.68 GeV/c. Nuclear parameters taken from inelastic electron scattering data. Dashed curve gives the cross section computed in the Born approximation. Data from Ref. 17).

Fig. 4. Same as Fig. 3 for the 9.6 (3^-) MeV level in C^{12}. The data is from Ref. 17) and is the sum of the 7.6 (0^+) + 9.6 (3^-) cross sections (see text for discussion).

Fig. 5. Inelastic electron scattering form factor for the 4.4 (2^+) level in C^{12}. Solid line was computed from the same nuclear model as in Fig. 3. Data from Ref. 15).

Fig. 6. Inelastic electron scattering form factor for the 9.6 (3^-_ level in C^{12}. Solid line was computed from the same nuclear model as in Fig. 4. Data from Ref. 15).

Fig. 7. Feynman diagrams for the Born approximation. Graphs a, b, and c contains s, t, and u channel poles, respectively.

Fig. 8. Cross section for π^+ production with 8.0 GeV/c photons on C^{12}. The dashed curve gives the computed cross section for only negative parity nuclear levels while the solid line

contains all levels. The dash-dot curve is the prediction of the Fermi gas model. The dotted ine gives the results of the Fermi gas model normalized to the data at $t = -0.169$ GeV/c and is presented to show more clearly the difference in momentum dependence between experiment and this simple model.

Fig. 9. Cross section for π^+ production with 8.0 GeV/c photons on C^{12} as functions of excitation energy for several values of momentum transfer. Only the largest cross sections are presented.

contains all levels. The dash-dot curve is the prediction of the Fermi gas model. The dotted ine gives the results of the Fermi gas model normalized to the data at $t = -0.169$ GeV/c and is presented to show more clearly the difference in momentum dependence between experiment and this simple model.

Fig. 9. Cross section for π^+ production with 8.0 GeV/c photons on C^{12} as functions of excitation energy for several values of momentum transfer. Only the largest cross sections are presented.

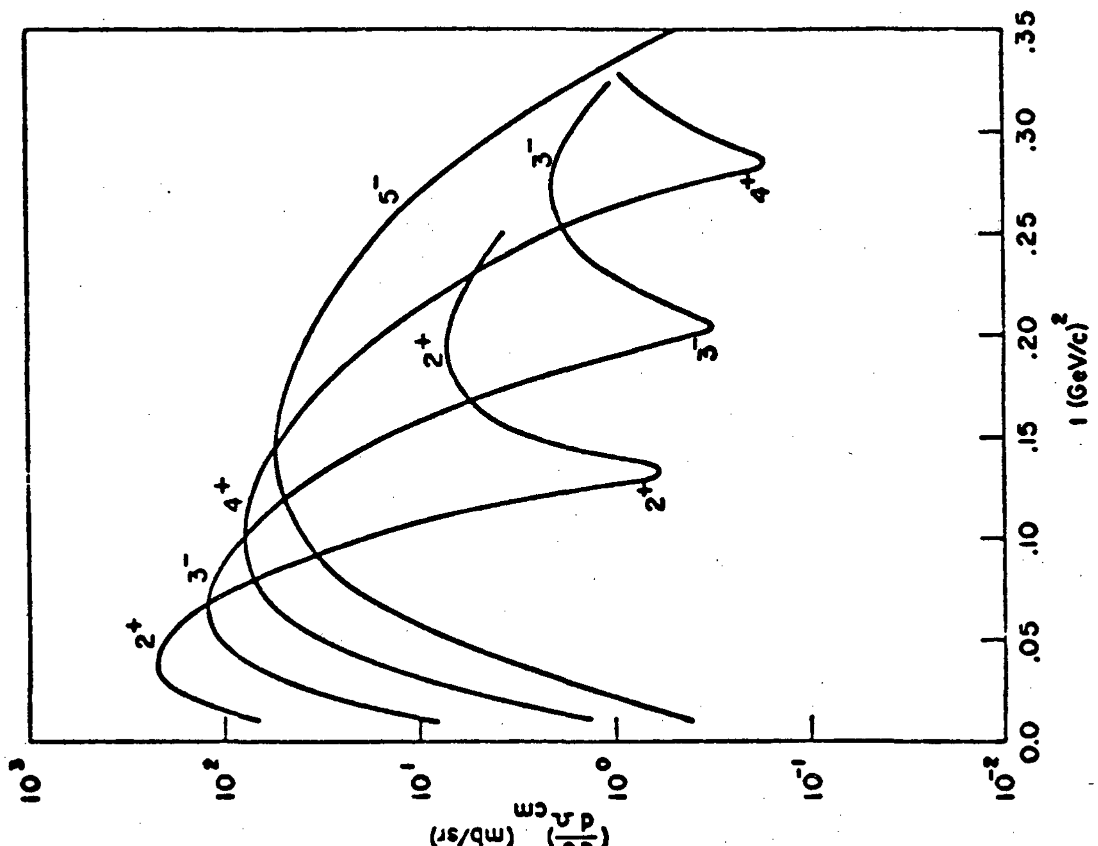

XBL 736-839

Fig. 1

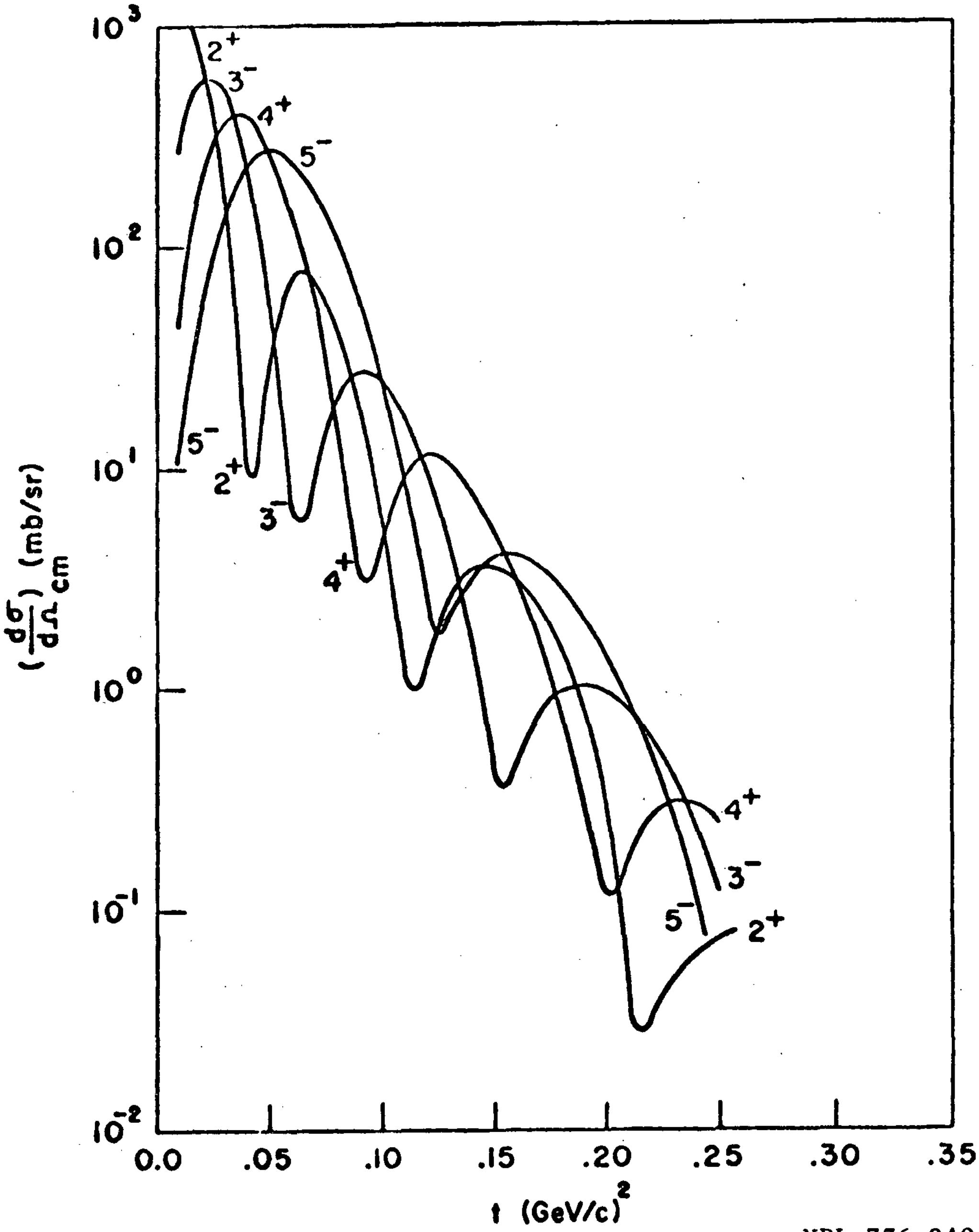

XBL 736-840

Fig. 2

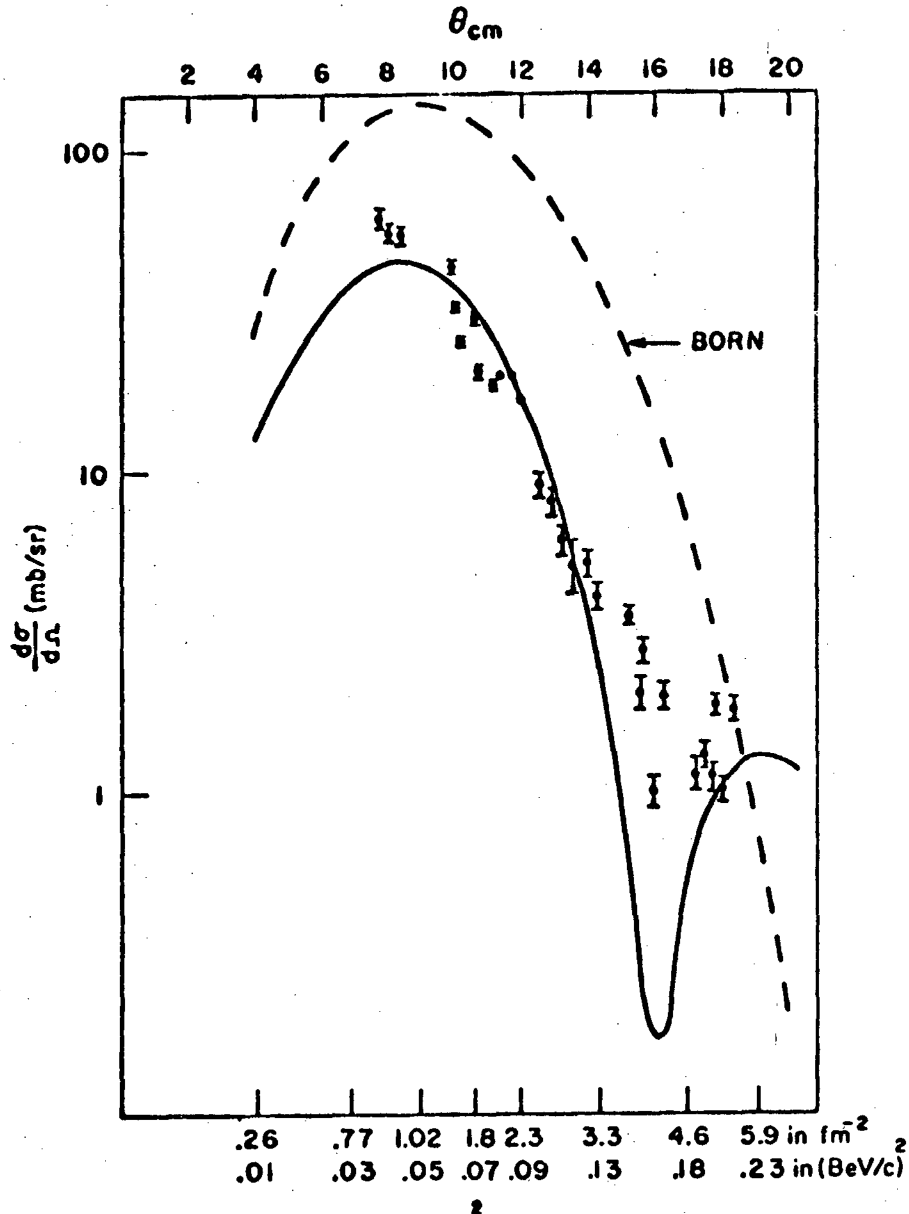

XBL 736-841

Fig. 3

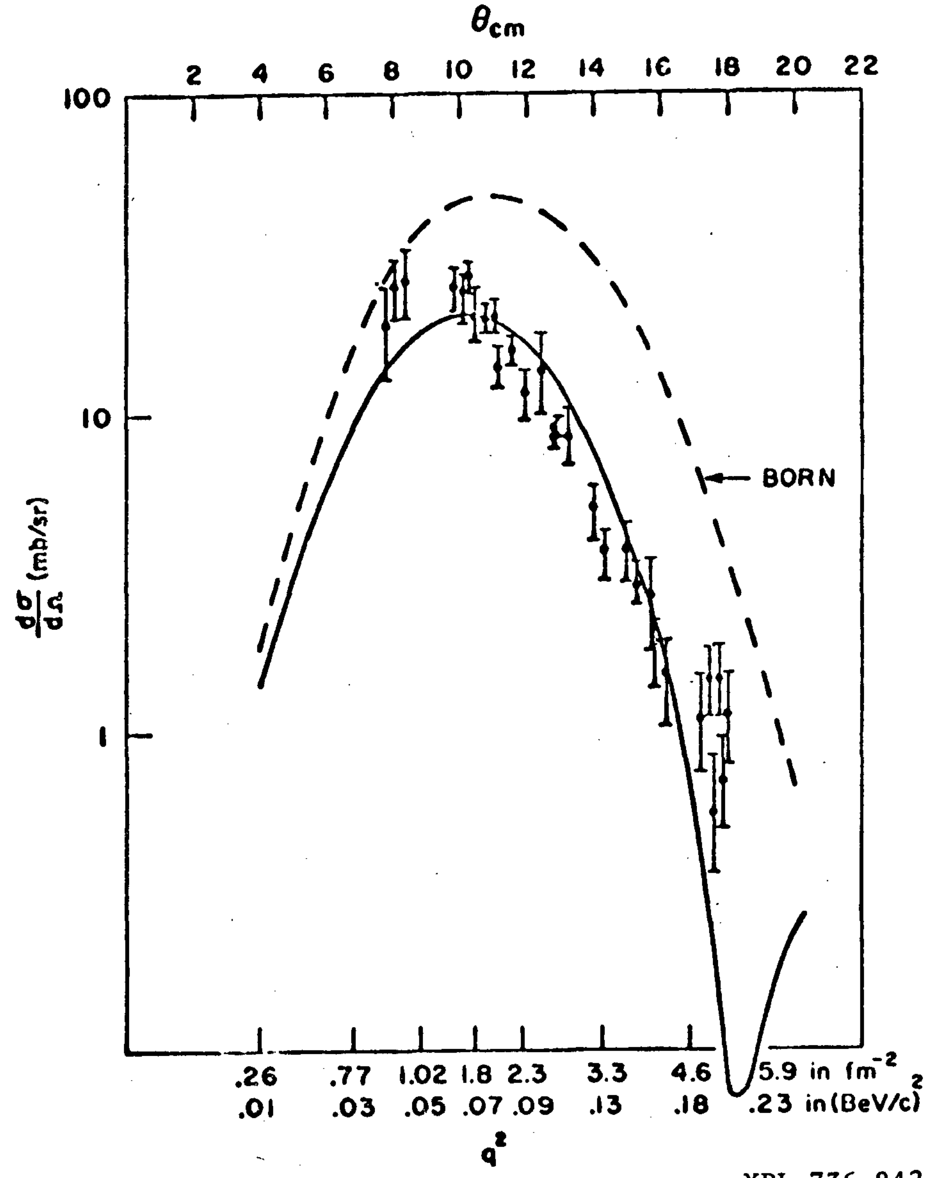

XBL 736-842

Fig. 4

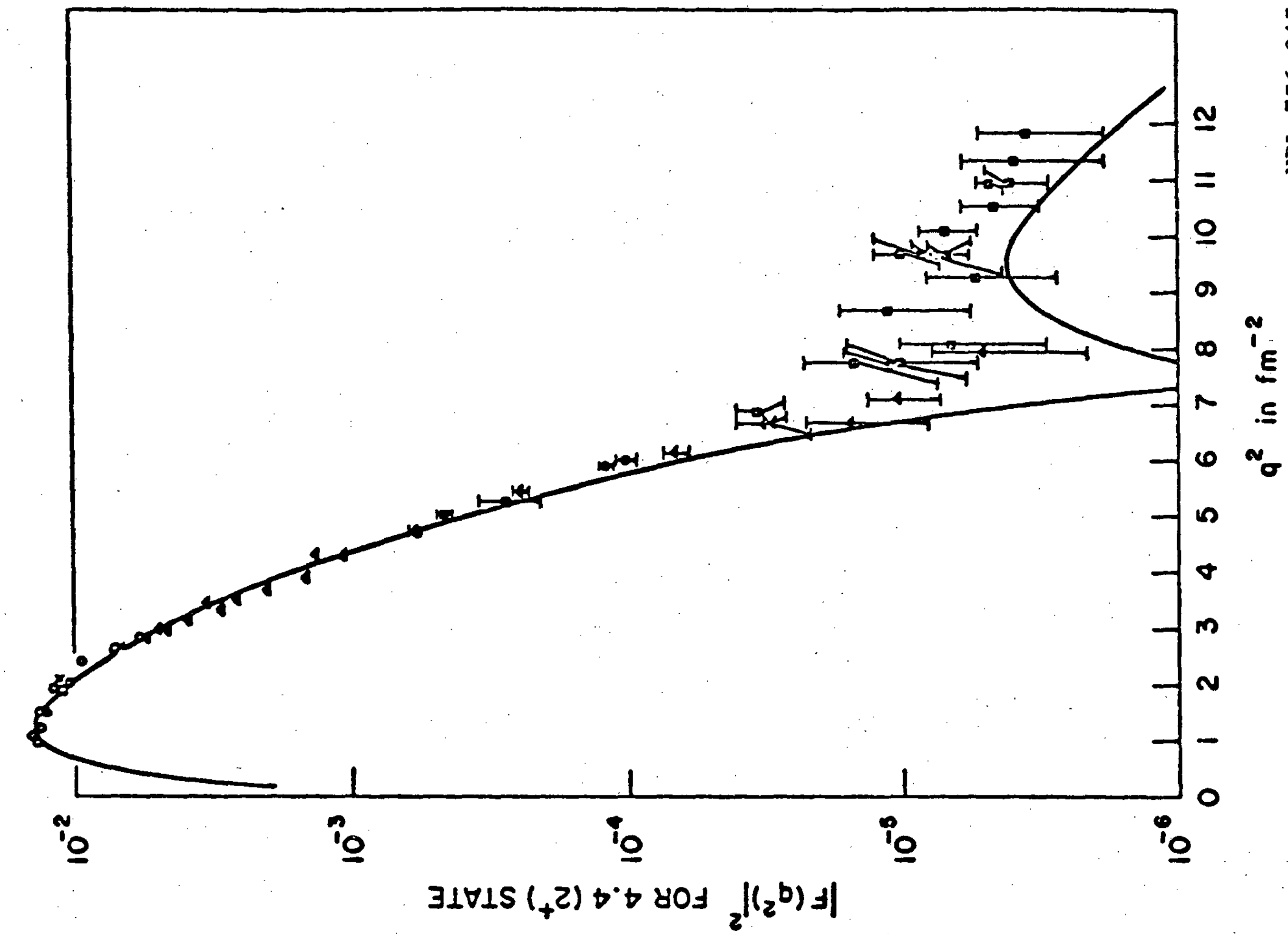

XBL 736-843

Fig. 5

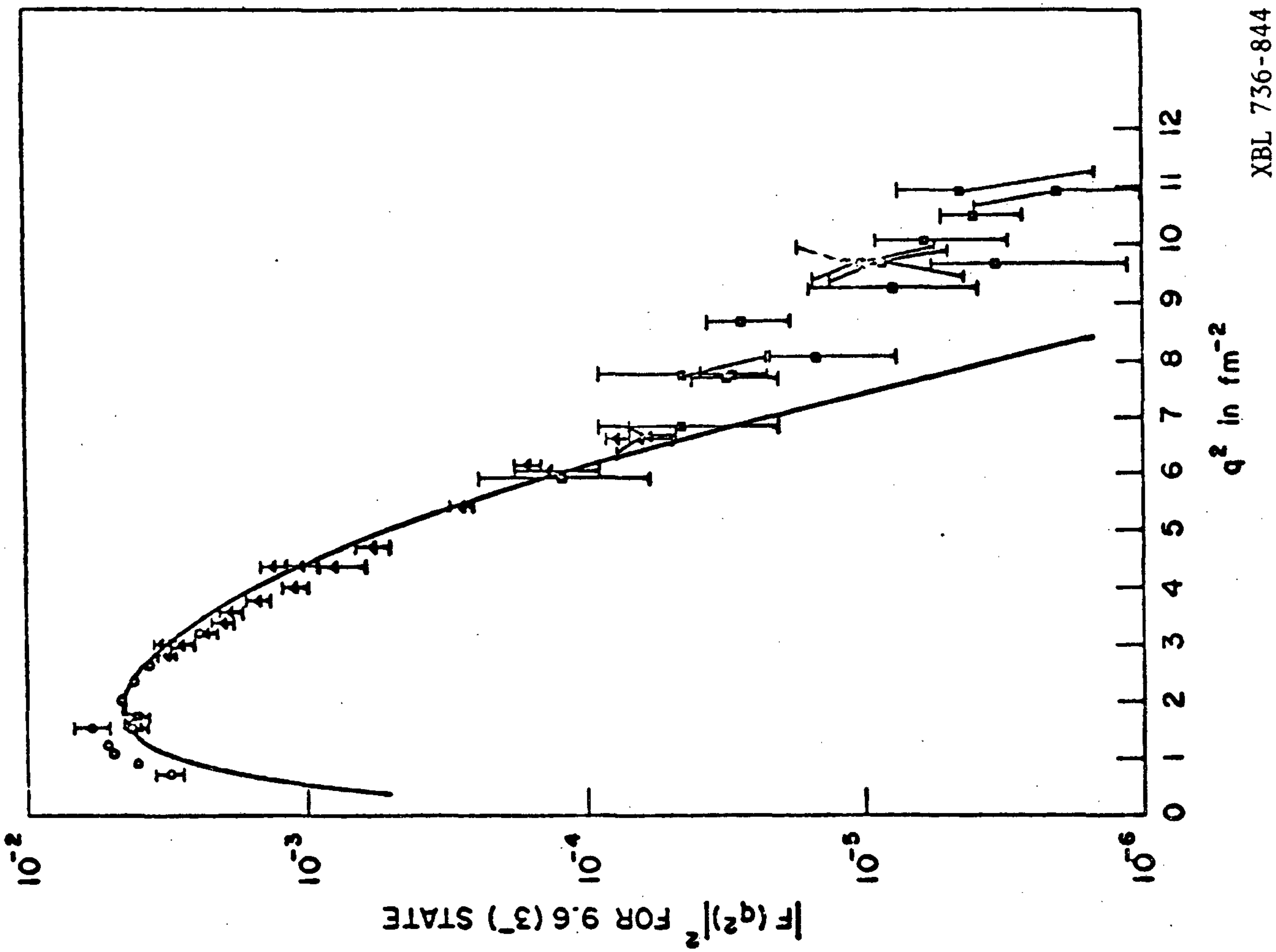

$|F(q^2)|^2$ FOR 9.6 (3⁻) STATE
10^{-2}
10^{-3}
10^{-4}
10^{-5}
10^{-6}
0 1 2 3 4 5 6 7 8 9 10 11 12
q^2 in fm^{-2}
XBL 736-844

Fig. 6

FEYNMAN GRAPHS USED TO DESCRIBE PION PHOTOPRODUCTION

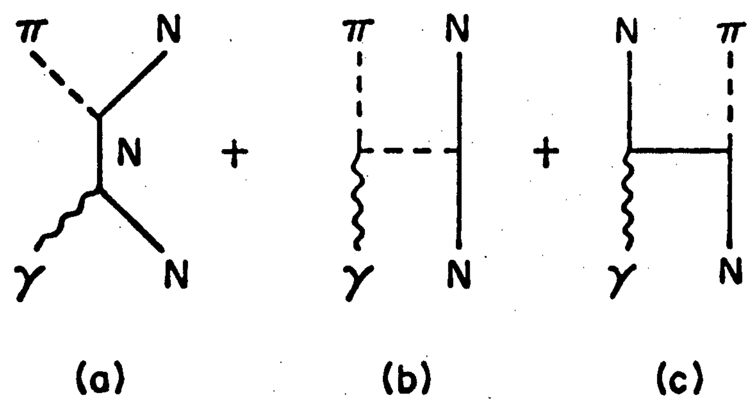

XBL 736-845

Fig. 7

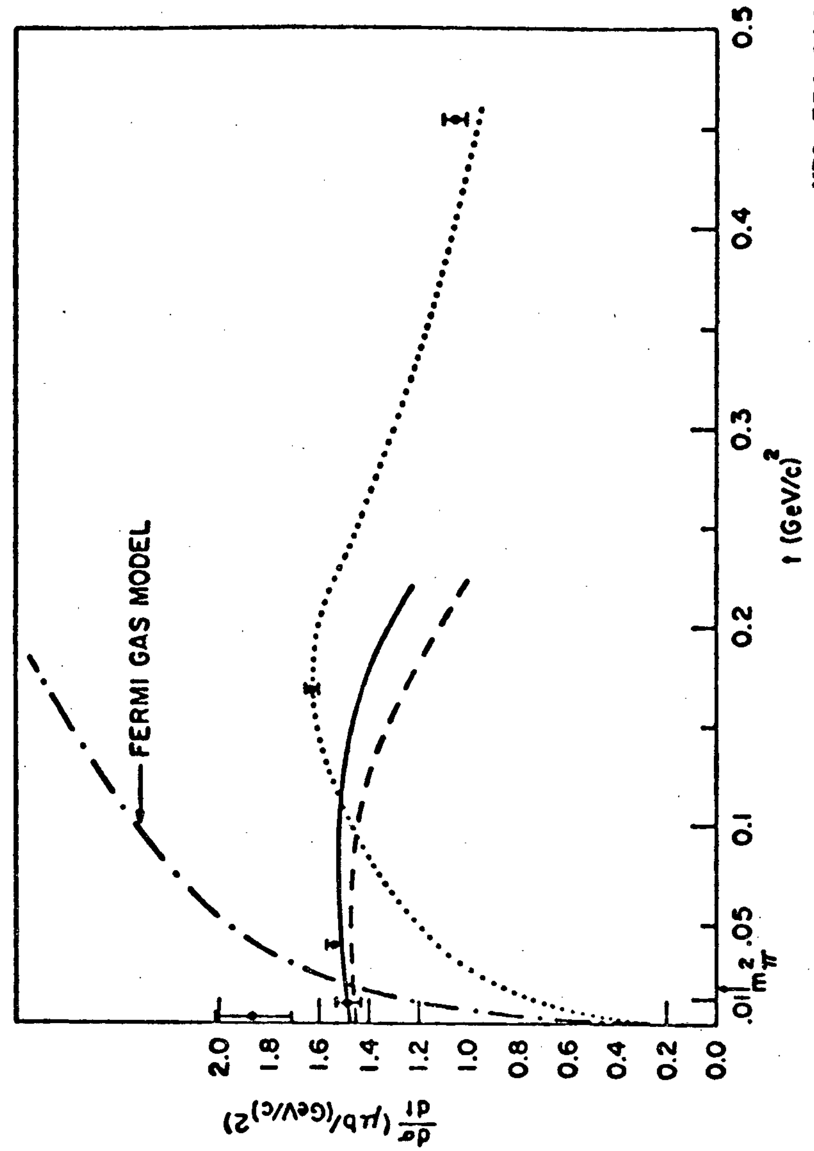

XBL 736-846

Fig. 8

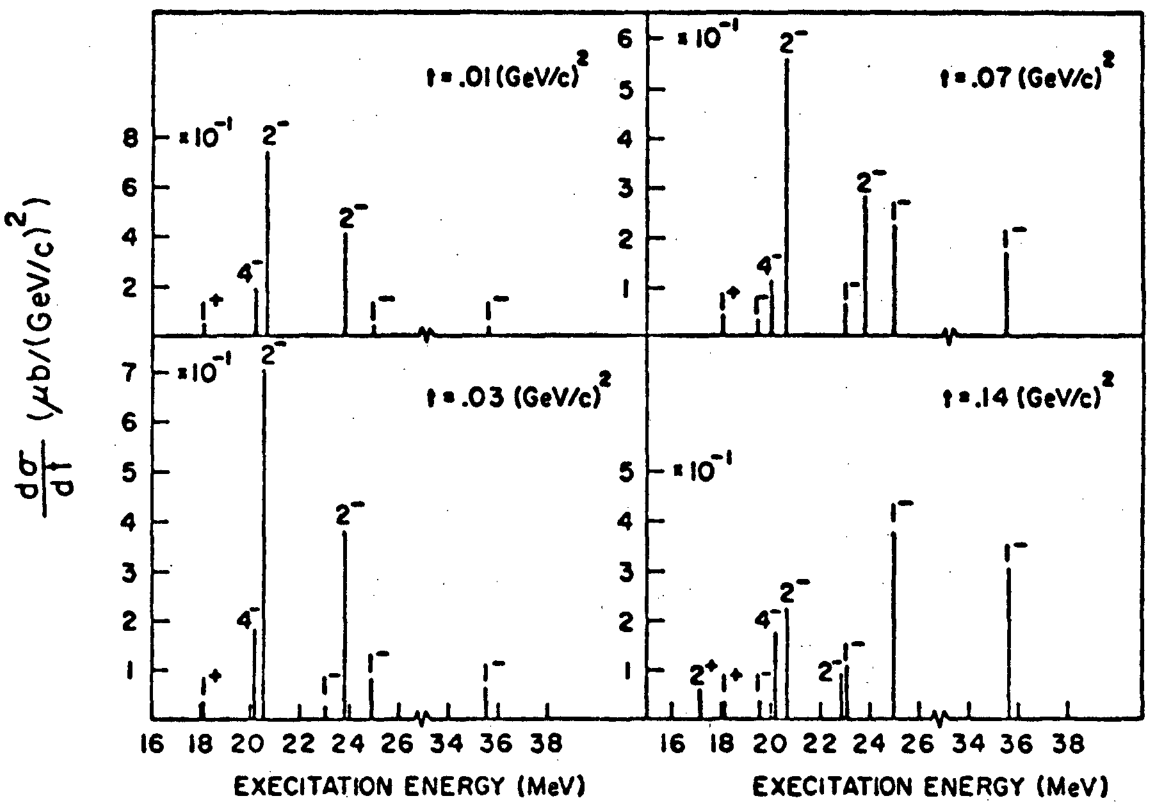

XBL 736-847

Fig. 9

LEGAL NOTICE

TECHNICAL INFORMATION DIVISION
LAWRENCE BERKELEY LABORATORY
UNIVERSITY OF CALIFORNIA
BERKELEY, CALIFORNIA 94720